Copyright © IFAC Automation in the Steel Industry,
Kyongju, Korea, 1997

A NEW ANTI-SWING CONTROL OF OVERHEAD CRANES

Ho-Hoon Lee *, Sung-Kun Cho,* and Jae-Sung Cho**

* *Process Automation Research Team,*
RIST, Pohang P.O. Box 135, Seoul 790-600, Korea
email: hhlee@risnet.rist.re.kr
** *Measurement and Control Team,*
POSLAB, Pohang P.O. Box 125, Seoul 790-600, Korea
email: gatsby@risnet.rist.re.kr

Abstract: This paper presents a new method for the design of an anti-swing control system for overhead cranes. The velocity servo system of a crane is modeled based on experiments. The model of the velocity servo system is used for the design of the position servo system of the crane via the loop shaping method. The position servo system and the swing dynamics of the crane load are then used to design the anti-swing control system based on the root locus method. In the presence of low frequency disturbances, the new anti-swing control system guarantees both zero steady state errors for position control and fast damping for load swing. Experimental results on a prototype crane show the effectiveness of the new anti-swing control system.
Copyright © 1998 IFAC

Keywords: anti-swing control, overhead crane, servo systems, root locus method, loop shaping method.

1. INTRODUCTION

Overhead cranes are widely used in factories, steelworks, and dockyards. A major problem with crane operation is that the acceleration of cranes induces unwanted load swing, which frequently causes damages to crane loads and even accidents; thus the crane operation usually requires intensive training. Accordingly, extensive researches have been performed to minimize the load swing in crane operation.

Mita and Kanai (1979) solved an optimal control problem for swing-free velocity profiles of a crane under the constraint of zero swing at the end of acceleration. Their method is an open loop control; thus it can not guarantee the control objective due to model uncertainties and disturbances. Ridout (1987) designed a linear feedback control law based on the root locus method. This method, however, does not guarantee zero steady state error for the position control of a crane. The load swing of a crane was also suppressed by setting the acceleration of the crane proportional to the angular velocity of the load swing (Yoon, *et al.*, 1995; Ohnish, *et al.*, 1981). Yamada et al. (1989) used swing-free velocity profiles and a fuzzy control law to suppress the position error of a crane and the load swing.

This paper proposes a new method for the design of an anti-swing control system, which guarantees not only fast damping for the load swing but also excellent transient responses and zero steady state error for the position control. First, the velocity servo dynamics of a crane is modeled based on experiments. Secondly, the position servo control system of the crane is designed based on the model of the velocity servo dynamics via the loop shaping method. Finally, the anti-swing control system is designed based on the position servo system and the swing dynamics of the crane load via the root locus method. In this study, the control laws and their gains are determined based on the experimental velocity servo dynamics of a crane and hence much effort can be saved in commissioning.

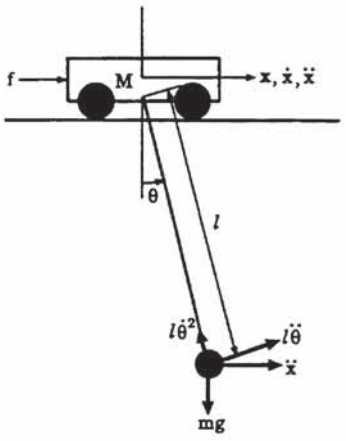

Fig. 1. A plane model of an overhead crane

This paper is organized as follows. In Section 2, the dynamic model of a crane is derived and then the velocity servo dynamics of the crane is obtained via the step response tests. In Section 3, the anti-swing control system is designed and its control performance is discussed. In Section 4, the results of experiments with a prototype overhead crane are presented to show the effectiveness of the anti-swing control system based on the proposed design method. Finally, the conclusion of this study is presented in Section 5.

2. MODELING

2.1 *Dynamic model of an overhead crane*

A plane model of a crane is shown in Fig. 1. In this study, the load is considered as a point mass, and the mass and the stiffness of the rope are neglected. In industry, the rope length is usually kept constant while the cranes are in motion for safety considerations. In this practical case, the equations of motion of the crane and the load can be derived as

$$(M+m)\ddot{x} + D\dot{x} - ml\dot{\theta}^2 \sin\theta + ml\ddot{\theta}\cos\theta = f, \quad (1)$$

$$ml^2\ddot{\theta} + mgl\sin\theta = -ml\ddot{x}\cos\theta, \quad (2)$$

where M and m represent the mass of the crane and the mass of the load, respectively; D is the viscous friction coefficient; θ, x, and l denote the swing angle, crane displacement, and rope length, respectively; f is the force applied to the crane.

In practice, the load swing is kept small for safety while the cranes are in motion. For small motions around the vertical equilibrium (i.e., $\theta \ll 1$), $\sin\theta \approx \theta$, $\cos\theta \approx 1$, and $\dot{\theta}^2 \approx 0$. In addition, most of industrial cranes are driven by high-ratio gear-reduction motors. Then $M \gg m$ holds and hence the $\ddot{\theta}$ term in (1) can be neglected (Ridout, 1987). Accordingly, for the practical cases the equations of motion are simplified as

$$M\ddot{x} + D\dot{x} = f, \quad (3)$$

$$\ddot{\theta} + \frac{g}{l}\theta = -\frac{\ddot{x}}{l}. \quad (4)$$

The Laplace transforms of (3) and (4) yield the following transfer functions:

$$\frac{V(s)}{F(s)} = \frac{1}{Ms+D}, \quad (5)$$

$$G_l(s) \equiv \frac{\Theta(s)}{X(s)} = \frac{-s^2/l}{s^2+g/l}, \quad (6)$$

where s is the Laplace operator; $X(s)$, $V(s)$, $F(s)$, and $\Theta(s)$ are the Laplace transforms of x, v, f, and θ, respectively, with $v = \dot{x}$.

2.2 *Modeling of the velocity servo system*

Most of automatic cranes are powered by AC servo motors with vector controllers. The dynamics of the vector controllers are in general a hundred times faster than those of the cranes. As a result, the dynamics of the vector controllers can be neglected in modeling. That is, the external force $F(s)$ can be written as

$$F(s) = K_m I_m(s) = K_t U_c(s), \quad (7)$$

where U_c is the input to the vector controller and I_m is the motor current; K_m and K_t are the constants that depend on the motor constants and the power train configuration of a crane. Then the equations (5) and (7) result in

$$G_t(s) \equiv \frac{V(s)}{U_c(s)} = \frac{K_t}{Ms+D}. \quad (8)$$

The velocity servo control system $G_v(s)$ is then obtained by setting $U_c(s) = K_v(s)(V_r(s) - V(s))$:

$$G_v(s) \equiv \frac{V(s)}{V_r(s)} = \frac{G_t(s)K_v(s)}{1+G_t(s)K_v(s)}, \quad (9)$$

where $V_r(s)$ represents the velocity command, and $K_v(s)$ is the velocity servo controller for which a PI (Proportional and Derivative) control is usually used.

In this study, the velocity servo dynamics $G_v(s)$ is obtained based on experiments. This will be described with a prototype crane built for this study. The prototype crane is driven by a geared AC servo motor whose angular velocity is controlled by a vector servo controller. Step commands are inputted to the vector servo controller, and then the velocity of the crane is measured as the output. From the input and output relations the velocity servo dynamics $G_v(s)$ can be modeled as

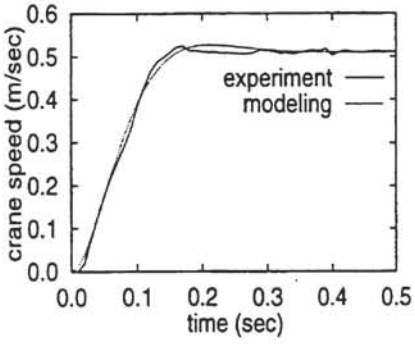

Fig. 2. Modeling of the velocity servo dynamics of the crane

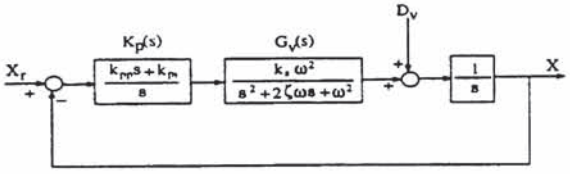

Fig. 3. Block diagram of the position servo system

$$G_v(s) = \frac{0.0567 \cdot 484}{s^2 + 32.6s + 484}. \tag{10}$$

Fig. 2 shows the step responses: the solid line for the experimental results and the dotted line for the theoretical results from the model (10).

3. CONTROL SYSTEM DESIGN

In this section, a position servo system will be designed, and then an anti-swing control system will be designed based on the position servo system and the swing dynamics $G_l(s)$. The velocity servo dynamics $G_v(s)$ of the prototype crane will be used for the design of the control systems.

3.1 *Design of the position servo system*

The position control loop is shown in Fig. 3. It consists of a position controller $K_p(s)$, the velocity servo dynamics $G_v(s)$, and an integrator $1/s$. An integration control is required to reject the effects of the disturbance D_v on the output X in the low frequency region. The slip of the crane wheels and the offsets of the vector servo controller are the examples of the disturbance.

In this paper, the loop shaping method (Doyle, *et al.*, 1992) is used for the design of the position controller $K_p(s)$. Fig. 4 shows the Bode plot of the open loop transfer function of the position servo system. The magnitude of the open loop transfer function is made sufficiently large in the low frequency region for good command tracking and disturbance rejection. In the high frequency region the open loop transfer function is made sufficiently

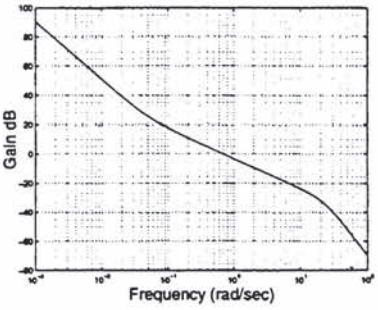

Fig. 4. Bode plot of the open loop transfer function of the position servo system

small for robust stability and sensor noise attenuation. The crossover frequency is selected in consideration of the bandwidth of the velocity servo dynamics $G_v(s)$ and uncertainties in the modeling. Around the crossover frequency the magnitude maintains a gentle slope (-20dB/dec) for a sufficient phase margin. The resulting open loop transfer function $G_{xo}(s) = K_p(s)G_v(s)/s$ is given as

$$G_{xo}(s) = \frac{329.3(s + 0.05)}{s^2(s^2 + 32.6s + 484)}. \tag{11}$$

From this, the controller $K_p(s)$ can be obtained as

$$K_p(s) = \frac{s \cdot G_{xo}(s)}{G_v(s)} = \frac{k_{pp}(s + k_{pi}/k_{pp})}{s}, \tag{12}$$

where the control gains k_{pp} and k_{pi} are 12.0 and 0.6, respectively. The position servo system $G_x(s)$ is then given as

$$G_x(s) \equiv \frac{X}{X_r} = \frac{329.3}{(s + 0.054)(s + 0.66)} \times \frac{(s + 0.05)}{(s^2 + 31.8s + 461.3)}. \tag{13}$$

3.2 *Design of the anti-swing control system*

Fig. 5 shows the block diagram of the anti-swing control system, which consists of the position servo system $G_x(s)$, an angle controller $K_a(s)$, and the load swing dynamics $G_l(s)$. Note that $s/(k_{pp}s + k_{pi})$ of $K_a(s)$ is canceled by $(k_{pp}s+k_{pi})/s$ of $K_p(s)$; thus, the feedback of the swing angle Θ to $G_v(s)$ (i.e., to the vector servo controller) constitutes a simple PD (Proportional and Derivative) control.

The bandwidth of $G_x(s)$ for most industrial cranes is usually smaller than the swing frequency $\sqrt{g/l}$. Therefore the dynamics of $G_x(s)$ should be taken into account when the angle controller $K_a(s)$ is designed.

In this paper, the angle controller $K_a(s)$ is designed via the root locus method. The zeros of

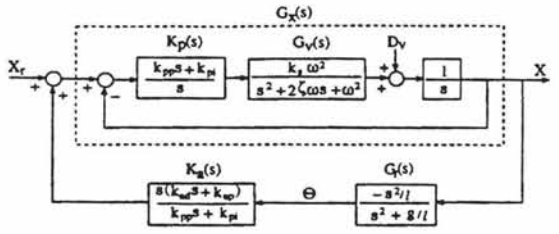

Fig. 5. Block diagram of the anti-swing control system

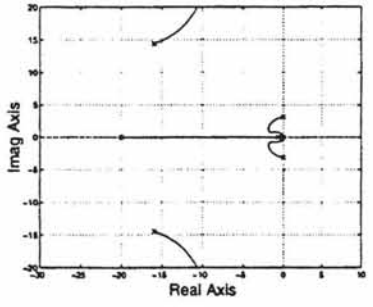

Fig. 6. Root locus of the anti-swing control system

$K_a(s)$ are placed at $s = 0$, $s = -k_{ap}/k_{ad}$, and the pole is placed at $s = -k_{pi}/k_{pp}$ in consideration of the poles and zeros of $G_x(s)$ and $G_l(s)$. The resulting open loop transfer function $G_{\theta o}(s)$ is determined as

$$G_{\theta o}(s) = \frac{-(27.4/l)k_{ad}s^3}{(s^2 + 9.8/l)(s + 0.05)(s + 0.66)} \times \frac{(s + k_{ap}/k_{ad})}{(s^2 + 31.8s + 461.3)}. \quad (14)$$

Fig. 6 shows the root locus ($0 \leq k_{ad} < \infty$) for the case of $l = 1.0$ m, where $k_{ap}/k_{ad} = 20.0$. Since two poles are placed on the real axis, the system is always stable regardless of the value of k_{ad}. The system, however, can be unstable for large k_{ad} owing to modeling errors in the high frequency region. The optimal values of k_{ad} having a damping ratio of 0.7 are 3.1 and 3.9 for $l = 1.0$ m and $l = 1.5$ m, respectively.

3.3 *System stability and performance*

The entire control system is stable since it has been stabilized based on the stable position servo system $G_x(s)$. In this section, the control performance of the entire control system is examined by using the transfer functions from each input to each output in Fig. 5. The transfer functions for $l = 1.0$ m can be derived as

$$\frac{X(s)}{X_r(s)} = \frac{27.4(s^2 + 9.8)(12s + 0.6)}{G_c(s)}, \quad (15)$$

$$\frac{\Theta(s)}{X_r(s)} = \frac{-27.4s^2(12s + 0.6)}{G_c(s)}, \quad (16)$$

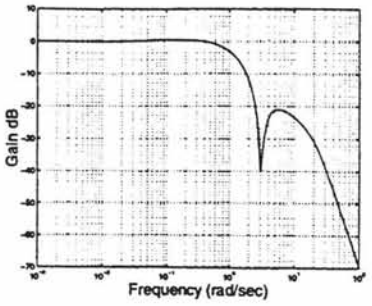

Fig. 7. Bode plot of the closed loop position control system X/X_r

$$\frac{X(s)}{D_v(s)} = \frac{s(s^2 + 9.8)(s^2 + 32.6s + 484)}{G_c(s)}, \quad (17)$$

$$\frac{\Theta(s)}{D_v(s)} = \frac{-s^3(s^2 + 32.6s + 484)}{G_c(s)}, \quad (18)$$

where $G_c(s)$ is defined as

$$G_c(s) \equiv (s + 0.05)(s^2 + 3.56s + 6.33) \times (s + 1.07)(s^2 + 27.9s + 437.8), \quad (19)$$

and $G_c(s) = 0$ is the characteristic equation of the closed loop system.

The transfer functions (15) $\sim$ (18) are all stable as expected. Fig. 7 is the Bode plot for X/X_r of (15), which shows excellent command tracking in the low frequency region. The bandwidth of X/X_r is about 1(rad/sec). The notch in X/X_r is due to the swing dynamics of the load. Θ/X_r of (16) shows that the swing angle is zero in the steady state for step or ramp position commands. According to X/D_v of (17) and Θ/D_v of (18), step disturbances have no effect on the crane position and the swing angle in the steady state. Furthermore, the steady state swing angle is not affected by ramp or parabola disturbances.

4. EXPERIMENTAL RESULTS

A prototype crane has been built to evaluate the control performance of the new anti-swing control system. The prototype crane is 5.5 meters long and 2 meters high. The maximum acceleration, speed, and rope length have been chosen such that the dynamics of the prototype crane is similar to that of an industrial overhead crane. The configuration of the prototype crane system is shown in Fig. 8.

The prototype crane is driven by an AC servo motor. If the encoder in the AC servo motor is to be used for measurements of the crane position, the slip of the crane wheels usually causes position errors. In this study, a precision position sensor has been designed. An angle sensor has been also designed and mounted on the bottom of the crane as shown in Fig. 8.

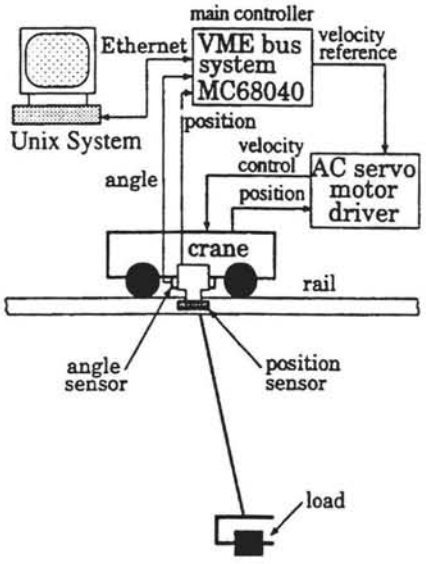

Fig. 8. Configuration of the experimental setup

The controller is composed of VMEbus systems: MC68040 CPU, analogue to digital, digital to analogue, and digital input/output boards. A commercial real-time operating system is used for the VMEbus control system. A Unix workstation is also used as the development host and is connected to VMEbus system through a private Ethernet LAN.

The designed control laws have been implemented through the VMEbus CPU board with 10 msec sampling period. Extensive control experiments have been performed under various conditions. In this paper, the experimental results with $l = 1.0$ m are discussed. The desired trajectories for the crane have been obtained based on the swing-free velocity profiles proposed by Mita and Kanai (1979). Since the control gains have been obtained based on the experimental velocity servo dynamics of the prototype crane, much effort could be saved in commissioning.

Fig. 9 and Fig. 10 show the experimental results for short and long crane displacements, respectively. The control performance is shown to be independent of the length of the crane displacement. The experimental result with $m = 20$ Kg is shown in Fig. 11. The experimental conditions for Fig. 10 and Fig. 11 are the same except for the load mass; the control performance is not affected by the load mass for the cranes powered by high-ratio gear-reduction motors.

The experimental result with about 10° initial swing is shown in Fig. 12. The position control is little affected by the initial swing. In all the experimental results, the steady state position errors are all zero, and the load swing disappears about 2 seconds after the crane reaches the desired positions even with the 10° initial load swing.

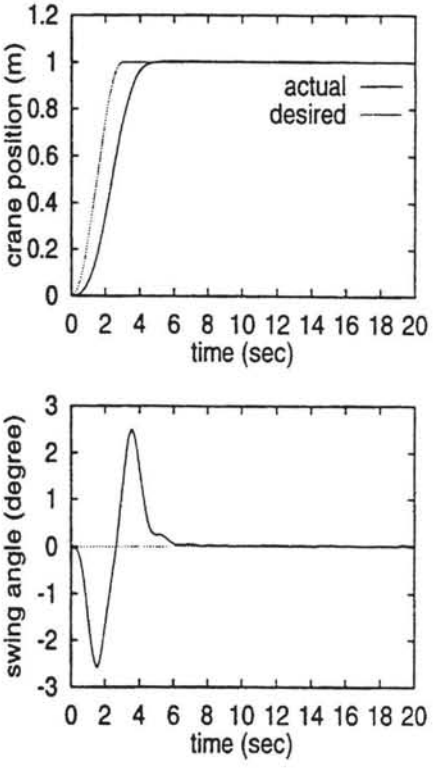

Fig. 9. Experimental results for a short crane displacement

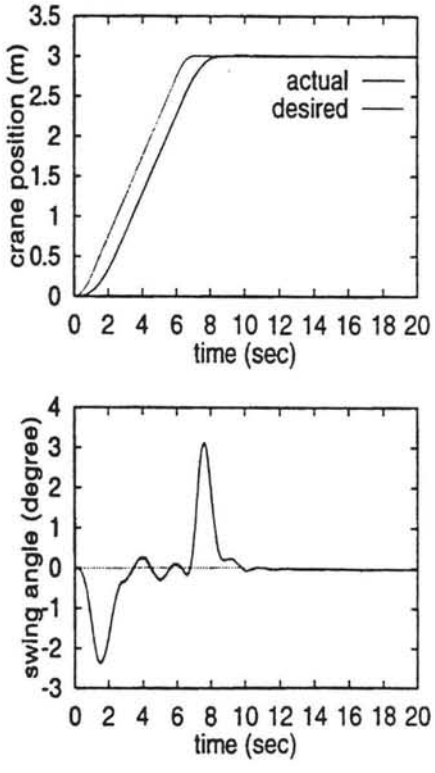

Fig. 10. Experimental results for a long crane displacement

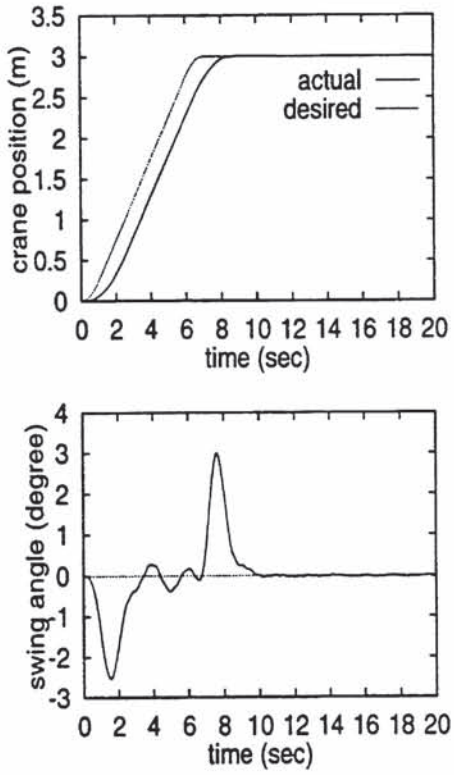

Fig. 11. Experimental results with $m = 20$ Kg

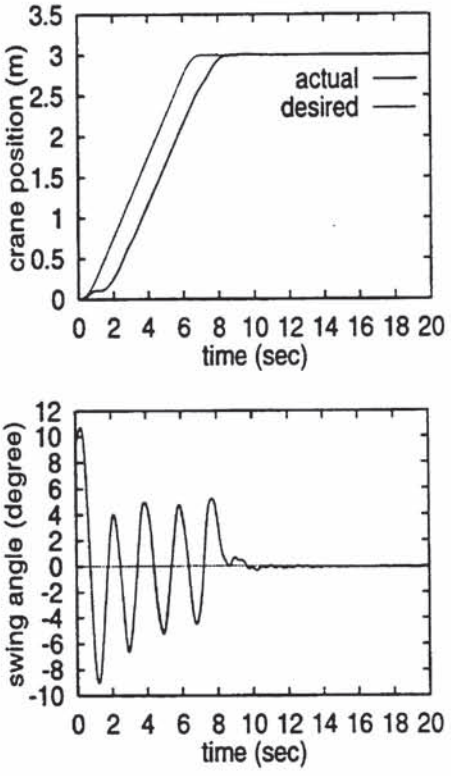

Fig. 12. Experimental results with 10° initial load swing

5. CONCLUSION

In this paper, a new design method has been presented; a new anti-swing control system has been designed based on the experimental velocity servo dynamics of a crane and the swing dynamics of the crane load. The new anti-swing control system guarantees zero steady state error and excellent transient responses for the position control of the crane. The new anti-swing control system also guarantees fast damping for load swing. Experimental results under various conditions have supported the above theoretical results.

Since the control laws and their gains have been determined by the experimental velocity servo dynamics of the crane, much effort could be saved in commissioning. Thus, the proposed design method and the resulting control laws have much potential for industrial applications.

In this study, the rope length is assumed to be constant while the cranes are in motion. In some applications, however, the rope length may be slowly time-varying. In future work, 'a gain scheduling method' will be used for the compensation of the changes in the rope length; an angle gain table for various rope lengths will be derived and will be used afterwards in the real-time control depending on the rope length. The position control is independent of the rope length.

6. REFERENCES

Mita, T. and T. Kanai (1979). Optimal Control of the Crane System Using the Maximum Speed of the Trolley (in Japanese with English abstract). *Trans. Soc. Instrum. Control Engr*, **Vol. 15, No. 6**, pp. 833-838.

Ridout, A. J. (1987). New Feedback Control System for Overhead Cranes. *Electric Energy Conference, Adelaide*, pp. 135-140.

Yamada, S., H. Fujikawa, and Y. Wakasugi (1989). Fuzzy Control of the Roof Control. *IEEE Industrial Electronics Conference Proceedings, Philadelphia*, pp. 709-714.

Ohnish, E., I. Tsuboi, T. Egusa, and M. Uesugi (1981). Automatic Control of an Overhead Crane. *IFAC 8th Triennial World Congress, Kyoto, Japan*, pp. 1885-1890.

Yoon, J. S., B. S. Park, J. S. Lee, and H. S. Park (1995). Various Control Schemes for Implementation of the Anti-Swing Crane. *Proceedings of the ANS 6th Topical Meeting on Robotics and Remote Systems, Monterey, California*, pp. 472-479.

Doyle, J. C., B. A. Francis, and A. R. Tannenbaum (1992). *Feedback Control Theory*, Chapter 7, Macmillan Publishing Company, New York.